Probabilistically Guaranteed Path Planning for Safe Urban Air Mobility Using Chance Constrained RRT*

Pengcheng Wu*
University of California San Diego, La Jolla, CA, 92093
San Diego State University, San Diego, CA, 92182

Lin Li†
University of North Carolina at Chapel Hill, Chapel Hill, NC, 27599

Junfei Xie‡ and Jun Chen§
San Diego State University, San Diego, CA, 92182

Flying safety is a critical concern for the successful operation of urban air mobility. This paper proposes a novel path planning algorithm based on the Rapidly-exploring Random Tree Star (RRT*) in conjunction with chance constrained formulation to handle uncertain environmental obstacles. Chance constrained formulation for uncertain obstacles under Gaussian noise is developed by converting the probabilistic constraints into deterministic constraints equivalently. The probabilistically feasible region at every time step can be established through the simulation of the system state and the evaluation of probabilistic constraints. By combining chance constrained formulation with RRT* algorithm, our proposed strategy not only enjoys the benefits of sampling-based algorithms but also incorporates uncertainty into the formulation. Simulation results demonstrate that the proposed algorithm can generate probabilistically guaranteed collision-free paths for urban air mobility operations.

I. Introduction

The air traffic transportation system around metropolitan areas is becoming more congested with rapid growth of traffic demand [1], [2], urban air mobility (UAM) is now increasingly drawing great attention to serve as a safe and efficient alternative[3]. However, there are still many challenges which remain to be explored. One critical concern is that various uncertainties may be present in urban scenarios, such as location uncertainties due to various disturbances of the position service (e.g. GPS), which may highly increase the chance of infeasibility for urban operations based on the current collision avoidance system. Alternatively, it is expected that a probabilistically guaranteed feasible path can be identified under a given risk level of collision for the vehicle subject to distinct forms of uncertainty instead. Lower risk often leads to higher computational intensity and longer planning time and trajectories. Therefore, it is important to achieve a balance between the planning conservatism and the risk of infeasibility entailed by collision.

Several different forms of uncertainty are found in common path planning scenarios involving collision avoidance [4]–[6]. One named model uncertainty is derived from the vehicle itself. Another one is derived from the sensing uncertainty of environmental obstacles that need to be evaded by the vehicle. Prentice et al. considered a linear system subject to Gaussian process noise to achieve the desired probability of feasibility [7]. Pepy et al. sought guaranteed feasibility for a nonlinear system subject to bounded state uncertainty of the model [8]. In addition to model uncertainty, many existing works have also focused on the environmental sensing uncertainty. Luders et al. studied probabilistic robustness to both process noise and uncertain dynamic obstacles following deterministic trajectories [9], [10]. Aoude et al. discussed the path planning for autonomous robots operating amidst dynamic obstacles with uncertain motion patterns [11]. However, all the works above treated model uncertainty and environmental sensing uncertainty separately. As a comparison, a concept of relative uncertainty is introduced in this paper, which can reduce different forms of uncertainty to one common uncertainty through a transformation.

*Joint PhD Student, Department of Aerospace Engineering, Student Member AIAA, pwu@sdsu.edu,pcwupat@ucsd.edu
†MS Student, Department of Biostatistics, amandali@live.unc.edu
‡Assistant Professor, Department of Electrical and Computer Engineering, Member AIAA, jxie4@sdsu.edu
§Assistant Professor, Department of Aerospace Engineering, Member AIAA, jun.chen@sdsu.edu (Corresponding Author)

One way to model uncertainty while planning trajectories is through chance constraints, a probabilistic bound for collision with obstacles which means that the probability of constraint violation doesn't exceed a prescribed value [12]. The chance constrained formulation proposed by Blackmore et al. assumes that all the obstacles have known, static locations [13], [14]. Some extensions based on Blackmore's work have been further explored to extend the chance constrained optimization framework to consider other kinds of uncertainty, such as collision avoidance between uncertain agents [15]. Luders et al. incorporated within the formulation of the uncertainty combining system state distribution and location of dynamic obstacles [9]. However, those formulations only work for convex polygon obstacles, which are often very conservative. In contrast, we propose an exact chance constraints formulation applying to both model and environmental uncertainties, which is more generic and accurate than existing ones [16].

Rapidly-exploring Random Tree (RRT), an incremental sampling-based algorithm first proposed by LaValle, is intended for path planning problems that involve obstacles and differential constraints [4], [17]. Compared with traditional motion planning algorithms, like potential field method, mixed-integer linear program, the neural network method, etc., the RRT algorithm is able to implement collision checking for widespread sampling points in the state space without accurate modeling. RRT algorithm can be regarded as a component incorporated into the development of a variety of different planning algorithms. The path planned by RRT will not necessarily be optimal. Some improvements have also been made based on the variations of the original RRT algorithm [18], [19]. RRT*, popularized by Karaman and Frazzoli, is an optimized modified algorithm that aims to achieve a shortest path, whether by distance or other metrics. It guarantees the asymptotic optimality while maintaining a tree structure like the standard RRT algorithm [20]. However, those algorithms don't consider the chance constraints within its formulation, leading to the fact that it cannot be used to deal with uncertain obstacles directly. In this paper, by incorporating chance constraints establishment into the RRT* formulation, the proposed method not only inherits the computational advantage of sampling-based algorithms, but also guarantees probabilistic feasibility for the planned trajectory at every time step.

The remainder of this article is organized as follows. In section II, the statement of the problem explored in this paper is established. In section III, the chance constrained formulation which allows for both model and environmental uncertainty is fully discussed. In section IV, the chance constrained formulation is incorporated into the RRT* algorithm, and in turn the chance constrained RRT* algorithm is presented. In section V, the feasibility of the proposed algorithm is verified through numerical simulation. Finally, we conclude this article in section VI.

II. Problem Statement

Consider a linear time invariant system which is described as

$$\begin{aligned} \boldsymbol{x}_{t+1} &= \boldsymbol{A}\boldsymbol{x}_t + \boldsymbol{B}\boldsymbol{u}_t + \boldsymbol{\omega}_t \\ \boldsymbol{\omega}_t &\sim N(\boldsymbol{\mu}_{t0}, \boldsymbol{\Sigma}_0) \end{aligned} \tag{1}$$

where $\boldsymbol{x}_t \in \mathbb{R}^{n_x}$ represents the system state vector, $\boldsymbol{u}_t \in \mathbb{R}^{n_u}$ represents the system input vector and $\boldsymbol{\omega}_t \in \mathbb{R}^{n_x}$ represents a disturbance acting on the system. Also, $N(\boldsymbol{\mu}_{t0}, \boldsymbol{\Sigma}_0)$ represents a Gaussian distribution with a time-varying expectation $\boldsymbol{\mu}_{t0}$ and covariance $\boldsymbol{\Sigma}_0$. The system itself is subject to model uncertainty that is posed by the noise $\boldsymbol{\omega}_t$.

It is assumed that there are some constraints acting on the system, which take the following form

$$\boldsymbol{x}_t \in \neg\mathcal{X}_t \equiv \neg\big(\bigcup_{i=1}^{B} \mathcal{X}_{ti}\big) \quad \forall t \quad i = 1, \cdots, B \tag{2}$$

where the operator $\neg$ denotes the operation of set complement. B denotes the number of uncertain environmental obstacles. $\mathcal{X}_{ti}$ denotes the possible region of an obstacle i at time step t, entailed by the location uncertainty of the obstacle. Note that the time dependence of $\mathcal{X}_t$ allows for either static or dynamic environmental obstacles included in our discussion.

The possible region of an obstacle i at time step t under the assumption of Gaussian distribution can be described as

$$\begin{aligned} \mathcal{X}_{ti} &= \mathcal{X}_{ti}^{range} + \boldsymbol{c}_{ti} \quad \forall t \quad i = 1, \cdots, B \\ \boldsymbol{c}_{ti} &\sim N(\boldsymbol{\mu}_{ti}, \boldsymbol{\Sigma}_i) \end{aligned} \tag{3}$$

where the operator '+' denotes the operation of set translation. $\mathcal{X}_{ti}^{range}$ represents a safe range which depends on the velocity of each obstacle [21]. For simplicity, we can assume that the safe ranges in this article are all identical, that is, $\forall\, t, i \;\; \mathcal{X}_{ti}^{range} = \mathcal{X}^{range}$. The time-dependent random variable vector $\boldsymbol{c}_{ti}$ represents the center position of the ith obstacle at time step t. It obeys a Gaussian distribution $\boldsymbol{c}_{ti} \sim N(\boldsymbol{\mu}_{ti}, \boldsymbol{\Sigma}_i)$ with time-varying expectation $\boldsymbol{\mu}_{ti}$. All $\boldsymbol{c}_{ti}$ are assumed to be independent. Please note that for a dynamic obstacle whose center follows a known trajectory, the center location $\boldsymbol{c}_{ti} \sim N(\boldsymbol{\mu}_{ti}, \boldsymbol{\Sigma}_i)$. For a static obstacle whose center keeps static, $\boldsymbol{c}_{ti} \sim N(\boldsymbol{\mu}_{ti}, \boldsymbol{\Sigma}_i)$ is reduced to $\boldsymbol{c}_i \sim N(\boldsymbol{\mu}_i, \boldsymbol{\Sigma}_i)$.

The primary objective of the motion planning problem presented in this paper is to find a feasible path for an unmanned aerial vehicle (UAV) starting from the initial state to the goal domain $\mathcal{X}_{\text{goal}} \subseteq \mathbb{R}^{n_x}$ within minimum time. That is, to realize

$$\begin{aligned} &\lim_{t \to t_{\text{goal}}} \boldsymbol{x}_t \in \mathcal{X}_{\text{goal}} \\ &t_{\text{goal}} = \min \left\{ t : \boldsymbol{x}_t \in \mathcal{X}_{\text{goal}} \right\} \end{aligned} \tag{4}$$

while guaranteeing all the obstacle avoidance requirements are satisfied at each time step $t \in \{0, \ldots, t_{\text{goal}}\}$ with probability of at least p_{safe}.

III. Chance Constraints under Gaussian Uncertainty

In this section, a risk domain $\mathcal{D}_{ti}$ at a given risk level α can be captured through transforming the possible region $\mathcal{X}_{ti}$ presented in last section into deterministic ones equivalently. It can be utilized to ensure that the probability of collision with any obstacles for a given time step is less than a risk bound. In doing so, the uncertainty of obstacles found in common path planning scenarios is able to be incorporated within the chance constrained formulation. Furthermore, model uncertainty attributed to the vehicle itself can also be reduced to a common form of uncertainty within our chance constraints formulation through the introduction of the notion of relative uncertainty.

Each obstacle is assumed to be distributed as a two dimensional Gaussian distribution. In other words, the location of each obstacle is represented through a random vector $\boldsymbol{X} = (x, y)^{\mathrm{T}}$, whose probability distribution is Gaussian with certain expectation and covariance values. The probability density function (PDF) of $\boldsymbol{X}$ is defined as [22],

$$f(\boldsymbol{X}) = \frac{1}{(2\pi)|\boldsymbol{\Sigma}|^{1/2}} \exp\left[-\frac{1}{2}(\boldsymbol{X}-\boldsymbol{\mu})^{\mathrm{T}}\boldsymbol{\Sigma}^{-1}(\boldsymbol{X}-\boldsymbol{\mu})\right] \tag{5}$$

where
$\boldsymbol{X} = (x, y)^{\mathrm{T}}$, a random vector with two random variables as components
$\boldsymbol{\mu} = (\mu_1, \mu_2)^{\mathrm{T}}$, a vector which denotes the expectation values of two random variables respectively
$\boldsymbol{\Sigma} = [\sigma_{11}\ \sigma_{12};\ \sigma_{21}\ \sigma_{22}]$, a symmetric positive definite matrix termed the covariance matrix. Note that the elements σ_{11} and σ_{22} represent the variances of two variables respectively, while σ_{12} or σ_{21} represents the correlation coefficients between those two variables. Moreover, if $\sigma_{12} > 0$, the random variables x and y are positively correlated; if $\sigma_{12} < 0$, they are negatively correlated; otherwise, they are definitely not correlated.

Assume that $\boldsymbol{X}$ is a random variable vector with the size of 2×1, which obeys a 2-dimensional Gaussian distribution $N(\boldsymbol{\mu}, \boldsymbol{\Sigma})$. As $\boldsymbol{X} \sim N(\boldsymbol{\mu}, \boldsymbol{\Sigma})$, then we have $(\boldsymbol{X}-\boldsymbol{\mu}) \sim N(\boldsymbol{0}, \boldsymbol{\Sigma})$. Thus, $T^2 = (\boldsymbol{X}-\boldsymbol{\mu})^{\mathrm{T}}\boldsymbol{\Sigma}^{-1}(\boldsymbol{X}-\boldsymbol{\mu}) \sim \chi_2^2$, where T^2 is a random scalar and χ_2^2 stands for a chi-squared distribution with 2 degrees of freedom [23].

The cumulative distribution function (CDF) of χ_2^2 is

$$F(x, 2) = \frac{\gamma(1, \frac{x}{2})}{\Gamma(1)} = P\left(1, \frac{x}{2}\right) \tag{6}$$

where $P\left(1, \frac{x}{2}\right)$ is the regularized gamma function. This CDF has a simple form

$$F(x) = 1 - e^{-\frac{x}{2}} \tag{7}$$

Because $F(x) : R^+ \to [0, 1)$ is a bijective mapping, we can find the inverse mapping for $F(x)$, which is defined as $F^{-1}(1-\alpha) : [0, 1) \to R^+$. The expression of the inverse mapping in terms of risk level α is χ^2value $= -2\ln(\alpha)$.

Given any risk level α, we can find a χ^2 value $F^{-1}(1-\alpha)$ such that $\Pr\left(T^2 > F^{-1}(1-\alpha)\right) = \alpha$. Therefore, $T^2 = (\boldsymbol{X}-\boldsymbol{\mu})^{\mathrm{T}}\boldsymbol{\Sigma}^{-1}(\boldsymbol{X}-\boldsymbol{\mu}) = F^{-1}(1-\alpha)$ forms the boundary of the risk domain $\mathcal{X}_{ti}$, which is derived from the Gaussian distribution of $\boldsymbol{X}$ at risk level α.

Recall that the expression $(\boldsymbol{X}-\boldsymbol{\mu})^{\mathrm{T}}\boldsymbol{\Sigma}^{-1}(\boldsymbol{X}-\boldsymbol{\mu})$ is a so-called quadratic form discussed in Linear Algebra [24]. Thus we have $\boldsymbol{X} \sim N(\boldsymbol{\mu}, \boldsymbol{\Sigma})$. Thus, $T^2 = (\boldsymbol{X}-\boldsymbol{\mu})^{\mathrm{T}}\boldsymbol{\Sigma}^{-1}(\boldsymbol{X}-\boldsymbol{\mu}) = F^{-1}(1-\alpha)$ can be geometrically interpreted as a circle or an ellipse, dependent on the given values of expectation $\boldsymbol{\mu}$ and covariance $\boldsymbol{\Sigma}$.

Therefore, the chance constraint for the vehicle attributed to a single uncertainty obstacle i at time step t is a quadratic inequality. Thus,

$$\begin{aligned} & \Pr(\text{collision}) \\ & \leq \Pr\big((\boldsymbol{X}-\boldsymbol{\mu})^{\mathrm{T}}\boldsymbol{\Sigma}^{-1}(\boldsymbol{X}-\boldsymbol{\mu}) > F^{-1}(1-\alpha)\big) \\ & \leq \alpha \end{aligned} \tag{8}$$

That is to say, given a risk level α which denotes the probability bound that the vehicle doesn't collide with any obstacle i at any time step t, we can transform the probabilistic region X_{ti} discussed in last section into a deterministic risk domain, which is geometrically represented as a circle or an ellipse.

For multiple obstacles, our objective is to ensure that the probability of collision with any obstacle i doesn't exceed a threshold value Δ. Those B Gaussian distributed obstacles are represented through the quadratic inequalities

$$\begin{aligned} & \vee\left(\left(\boldsymbol{x}_t-\boldsymbol{\mu}_i\right)^{\mathrm{T}}\boldsymbol{\Sigma}_i^{-1}\left(\boldsymbol{x}_t-\boldsymbol{\mu}_i\right) \leq F^{-1}(1-\alpha)\right) \\ & i=1,\cdots,B \end{aligned} \tag{9}$$

To avoid all the obstacles at each time step, the system must satisfy B quadratic inequalities at the same time

$$\begin{aligned} & \wedge\left(\left(\boldsymbol{x}_t-\boldsymbol{\mu}_i\right)^{\mathrm{T}}\boldsymbol{\Sigma}_i^{-1}\left(\boldsymbol{x}_t-\boldsymbol{\mu}_i\right) > F^{-1}(1-\alpha)\right) \\ & i=1,\cdots,B \end{aligned} \tag{10}$$

Consider the problem of avoiding the ith obstacle on the tth time step. To avoid the obstacles with a risk probability less than α , it is necessary to not satisfy any one of the quadratic inequalities given in eq. (9). Conversely, any violation of the quadratic inequalities inequalities given in eq. (10) will lead to the failure of collision avoidance. In fact, it is the case that

$$\begin{aligned} & \Pr(\text{collision}) \\ & = \Pr\left(\vee\left(\left(\boldsymbol{x}_t-\boldsymbol{\mu}_i\right)^{\mathrm{T}}\boldsymbol{\Sigma}_i^{-1}\left(\boldsymbol{x}_t-\boldsymbol{\mu}_i\right) \leq F^{-1}(1-\alpha)\right)\right) \\ & = \sum_{i=1}^{B}\Pr\left(\left(\boldsymbol{x}_i-\boldsymbol{\mu}_i\right)^{\top}\boldsymbol{\Sigma}_i^{-1}\left(\boldsymbol{x}_i-\boldsymbol{\mu}_i\right) \leq F^{-1}(1-\alpha)\right) \\ & - \Pr\left(\wedge\left(\left(\boldsymbol{x}_i-\boldsymbol{\mu}_i\right)^{\mathrm{T}}\boldsymbol{\Sigma}_i^{-1}\left(\boldsymbol{x}_i-\boldsymbol{\mu}_i\right) \leq F^{-1}(1-\alpha)\right)\right) \\ & \leq \sum_{i=1}^{B}\Pr\left(\left(\boldsymbol{x}_t-\boldsymbol{\mu}_i\right)^{\mathrm{T}}\boldsymbol{\Sigma}_i^{-1}\left(\boldsymbol{x}_t-\boldsymbol{\mu}_i\right) \leq F^{-1}(1-\alpha)\right) \\ & i=1,\ldots,B \end{aligned} \tag{11}$$

To ensure that the probability of collision is less than α, it is only required to show that the significance level of the Gaussian distribution is satisfied with

$$\begin{aligned} & \Pr(\text{collision}) \\ & \leq \sum_{i=1}^{B}\Pr\Big((\boldsymbol{x}_t-\boldsymbol{\mu}_i)^{\mathrm{T}}\boldsymbol{\Sigma}_i^{-1}(\boldsymbol{x}_t-\boldsymbol{\mu}_i) \leq F^{-1}(1-\alpha)\Big) \\ & \leq B\alpha \leq \Delta \qquad i=1,\ldots,B \end{aligned} \tag{12}$$

According to the discussion above, the probabilistic collision avoidance can be satisfied on condition that the planned paths of the vehicles system don't intersect with the risk domain of the B obstacles at the risk level α satisfying probability inequality $B\alpha \leq \Delta$.

So far we only considered the scenario where only obstacle uncertainty exists. Through introducing the notion of relative uncertainty which combines both model uncertainty and environmental obstacle uncertainty, the risk domain theory can also be smoothly extended to work for scenarios where both two forms of uncertainty exist.

Suppose that a random variable

$$\boldsymbol{X} \sim N\Big((\mu_1,\mu_2)^{\mathrm{T}}, \begin{bmatrix} \sigma_{11} & \sigma_{12} \\ \sigma_{21} & \sigma_{22} \end{bmatrix}\Big) \tag{13}$$

denotes the center location of the vehicle, and another random variable

$$\boldsymbol{Y} \sim N\big((v_1, v_2)^{\mathrm{T}}, \begin{bmatrix} \tau_{11} & \tau_{12} \\ \tau_{21} & \tau_{22} \end{bmatrix}\big) \tag{14}$$

denotes the center location of the environmental obstacle. Then we can find that a relative random variable $\boldsymbol{Z} = (\boldsymbol{X} - \boldsymbol{Y})$ obeys a new Gaussian distribution, that is

$$\begin{aligned} \boldsymbol{Z} &\sim N\big(\boldsymbol{\mu}, \boldsymbol{\Sigma}\big) \\ &\sim N\big(\mathrm{E}(\boldsymbol{X} - \boldsymbol{Y}), \mathrm{var}(\boldsymbol{X} - \boldsymbol{Y})\big) \end{aligned} \tag{15}$$

where the expectation and covariance of $\boldsymbol{Z} = (\boldsymbol{X} - \boldsymbol{Y})$ are represented by

$$\begin{aligned} \boldsymbol{\mu} &= \mathrm{E}(\boldsymbol{X} - \boldsymbol{Y}) \\ &= \mathrm{E}(\boldsymbol{X}) - \mathrm{E}(\boldsymbol{Y}) \\ &= (\mu_1 - v_1, \mu_2 - v_2)^{\mathrm{T}} \\ \boldsymbol{\Sigma} &= \mathrm{var}(\boldsymbol{X} - \boldsymbol{Y}) \\ &= \mathrm{var}(\boldsymbol{X}) + \mathrm{var}(\boldsymbol{Y}) - 2\rho\sqrt{\mathrm{var}(\boldsymbol{X})\,\mathrm{var}(\boldsymbol{Y})} \\ &= \begin{bmatrix} \sigma_{11} & \sigma_{12} \\ \sigma_{21} & \sigma_{22} \end{bmatrix} + \begin{bmatrix} \tau_{11} & \tau_{12} \\ \tau_{21} & \tau_{22} \end{bmatrix} \\ &- 2\rho\sqrt{\begin{bmatrix} \sigma_{11} & \sigma_{12} \\ \sigma_{21} & \sigma_{22} \end{bmatrix}\begin{bmatrix} \tau_{11} & \tau_{12} \\ \tau_{21} & \tau_{22} \end{bmatrix}} \end{aligned} \tag{16}$$

and ρ represents the correlation coefficient between the vehicle model and the environmental obstacle.

Likewise, the risk domain for the relative position $\boldsymbol{Z}$ between the ith obstacle center and the vehicle at time step t is

$$(\boldsymbol{Z} - \boldsymbol{\mu})^{\mathrm{T}}\boldsymbol{\Sigma}^{-1}(\boldsymbol{Z} - \boldsymbol{\mu}) = F^{-1}(1 - \alpha) \tag{17}$$

which is also a circle or an ellipse.

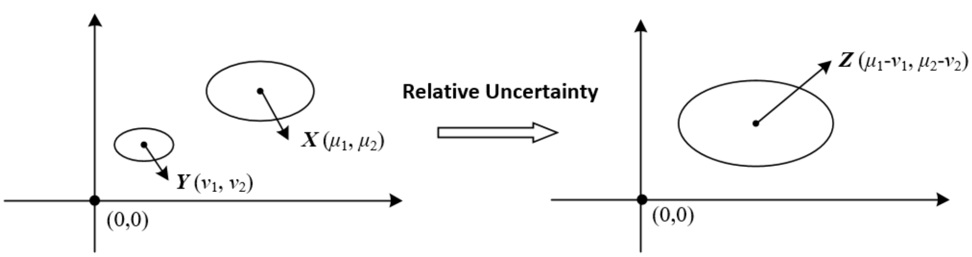

Fig. 1 Illustration of relative uncertainty transformation

According to the risk domain theory formulated above, we can also establish a risk domain for the relative random variable $\boldsymbol{Z} = (\boldsymbol{X} - \boldsymbol{Y})$, which is also a circle or an ellipse. To check whether the vehicle would collide with the environmental obstacle, it's only required to check the relative position between the origin $(0, 0)$ and the risk domain represented by a circle or an ellipse, as shown in Fig. 1. If the origin falls inside the risk domain, the probability of collision exceeds the prescribed risk bound

$$\begin{aligned} &\Pr(\text{collision}) \\ &\leq \Pr\big((\boldsymbol{Z} - \boldsymbol{\mu})^{\mathrm{T}}\boldsymbol{\Sigma}^{-1}(\boldsymbol{Z} - \boldsymbol{\mu}) > F^{-1}(1 - \alpha)\big) \\ &\leq \alpha \end{aligned} \tag{18}$$

Through the discussion of relative Gaussian uncertainty, we successfully transform both two forms of uncertainty into one common uncertainty, instead of dealing with two different forms of uncertainty independently.

IV. Chance Constrained RRT* Algorithm

In this section, the chance constrained RRT* algorithm (CC-RRT*) is developed as an extension of the standard RRT* algorithm by incorporating the chance constraints formulated in last section to handle uncertainties.

RRT* algorithm is a sampling-based motion planning algorithm intended for the efficient search for high dimensional space. Karaman et al. proved that for sampling-based motion planning algorithms, as the sampling points of RRT algorithm tend to infinity, the probability of its convergence to the optimal solution becomes zero[20]. Alternatively, they proposed RRT* algorithm which ensures the asymptotic optimality on the basis of the original RRT algorithm. This algorithm improves the way of parent node selection, and introduces the notion of cost function to select the node as the parent node which has the minimum cost within the neighborhood of the node extended. At the same time, nodes in the existing tree will be reconnected after each iteration, so as to ensure the computational complexity and asymptotic optimality.

Based on that, the chance constrained RRT* algorithm is considered as an extension of standard RRT* algorithm in the sense that it applies trajectory-wise constraints checking, allowing for the incorporation of probabilistic constraints. While standard RRT* algorithm grows a tree of states known to be feasible, CC-RRT* algorithm creates a tree of states satisfying probabilistic constraints subject to uncertain obstacles under a certain risk level. Fig. 2 illustrates that the proposed CC-RRT* algorithm grows a tree with the purpose of finding a path (red) which satisfies the probabilistic feasibility, connecting the start and goal points. The model uncertainty of the vehicle at each node is represented as an orange ellipse, and the environmental sensing uncertainty is represented as a grey ellipse. The vehicle's location at each node is checked against the constraints (grey ellipse). If the orange ellipse intersects with the grey ellipse, it means the probability of collision really exceeds a prescribed value and the current node should be discarded; otherwise, the current node should be reserved and may contribute to growing future paths.

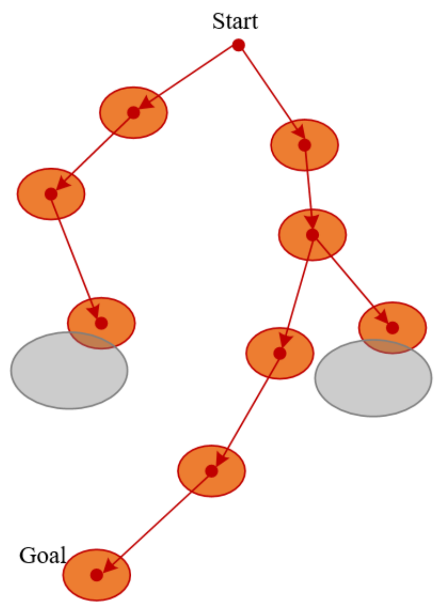

Fig. 2 Diagram of CC-RRT* planning

The steps of CC-RRT* planning intended for such a scenario are presented in **Algorithm 1**. It utilizes the chance constrained formulation developed in last section, which applies a fixed probability bound Δ/B across all obstacles, lead to deterministic constraints able to be computed at each time step. With the chance constraints formulation, one can determine whether equivalent deterministic constraints are satisfied or not through evaluating the relative position between a sample point $\boldsymbol{x}_{\text{rand}}$ and the corresponding risk domain $\mathcal{D}_i$ of obstacle i for all time steps at a given risk level α. The sample point $\boldsymbol{x}_{\text{rand}}$ is a node of the CC-RRT* tree that doesn't violate the risk domain $\mathcal{D}_i$. It is guaranteed that each node of the tree satisfies the probability bound of collision with any obstacle i through CC-RRT* planning.

Algorithm 1 Chance Constrained RRT* Planning

vertex $V \leftarrow \boldsymbol{x}_{\text{start}}$; edge $E \leftarrow \emptyset$; iteration step $k \leftarrow 0$
while $k < threshold$ **do** iteration implementation
  $G \leftarrow (V, E)$ generate a tree
  $\boldsymbol{x}_{\text{rand}} \leftarrow$ Sample( ) take a sample point from the environment
  $\boldsymbol{x}_{\text{nearest}} \leftarrow$ Nearest$(G, \boldsymbol{x}_{\text{rand}})$ identify the nearest node from the tree
  $\boldsymbol{x}_{\text{new}} \leftarrow$ Steer$(\boldsymbol{x}_{\text{nearest}}, \boldsymbol{x}_{\text{rand}})$ generate a new node out of the tree
  $\boldsymbol{p}_{\text{new}} \leftarrow$ Path$(\boldsymbol{x}_{\text{nearest}}, \boldsymbol{x}_{\text{new}})$ generate a new path between two nodes
  if CollisionFree$(\boldsymbol{p}_{\text{new}}, \mathcal{D}_i)$ evaluate the probability of collision
    $V \leftarrow V \cup \boldsymbol{x}_{\text{new}}$ add the new node to the tree
    $E \leftarrow E \cup \boldsymbol{p}_{\text{new}}$ add the new path to the tree
    $\boldsymbol{x}_{\text{min}} \leftarrow \boldsymbol{x}_{\text{nearest}}$
    $\boldsymbol{C}_{\text{near}} \leftarrow$ Near$(G, \boldsymbol{x}_{\text{new}}, |V|)$
    for all $\boldsymbol{x}_{\text{near}} \in \boldsymbol{C}_{\text{near}}$ **do**
      if CollisionFree$(\boldsymbol{x}_{\text{near}}, \boldsymbol{x}_{\text{new}})$ **then**
        $c' \leftarrow$ Cost$(\boldsymbol{x}_{\text{near}})$ + Line$(\boldsymbol{x}_{\text{near}}, \boldsymbol{x}_{\text{new}})$
        if $c' <$ Cost$(\boldsymbol{x}_{\text{new}})$ **then**
          $\boldsymbol{x}_{\text{min}} \leftarrow \boldsymbol{x}_{\text{near}}$
    $E' \leftarrow E' \cup \{(\boldsymbol{x}_{\text{min}}, \boldsymbol{x}_{\text{new}})\}$
    for all $\boldsymbol{x}_{\text{near}} \in \boldsymbol{C}_{\text{near}} \backslash \{\boldsymbol{x}_{\text{min}}\}$ **do**
      if CollisionFree$(\boldsymbol{x}_{\text{new}}, \boldsymbol{x}_{\text{near}})$ and Cost$(\boldsymbol{x}_{\text{near}})$
          $>$ Cost$(\boldsymbol{x}_{\text{new}})$ + Line$(\boldsymbol{x}_{\text{new}}, \boldsymbol{x}_{\text{near}})$ **then**
        $\boldsymbol{x}_{\text{parent}} \leftarrow$ Parent$(\boldsymbol{x}_{\text{near}})$
        $E' \leftarrow E' \backslash \{(\boldsymbol{x}_{\text{parent}}, \boldsymbol{x}_{\text{near}})\}$
        $E' \cup E' \backslash \{(\boldsymbol{x}_{\text{new}}, \boldsymbol{x}_{\text{near}})\}$
    if $|\boldsymbol{x}_{\text{new}} - \boldsymbol{x}_{\text{goal}}| < \delta$ check the proximity to the goal point
      break find a path feasible
    end if
  end if
  $k \leftarrow k + 1$ iteration step increases
end while

V. Simulation Results

In this section, several simulation cases are performed to verify the probabilistic feasibility of the proposed CC-RRT* algorithm using a single UAV.

All the obstacles in this section are assumed to be uncertain. The static obstacle is centered at $\boldsymbol{X}_{obs} = (x, y) \sim N(\boldsymbol{\mu}_{obs}, \boldsymbol{\Sigma}_{obs})$ with $\boldsymbol{\Sigma}_{obs} = [\frac{2}{3}\ 0;\ 0\ \frac{1}{6}]$. The position of the UAV is set to be $\boldsymbol{X}_{uav} = (x, y) \sim N(\boldsymbol{\mu}_{uav}, \boldsymbol{\Sigma}_{uav})$ with $\boldsymbol{\Sigma}_{uav} = [\frac{1}{24}\ 0;\ 0\ \frac{1}{96}]$, while the UAV's position is time-varying and determined by the nodes of path planned by the CC-RRT* at each time step t.

For a given risk level α in each case, the simulation is divided into two steps:

1. Planning with Algorithm 1

We first formulate chance constraints for every obstacle i at every time step t at the given risk level α. Then we run CC-RRT* algorithm 1 to find a path with the desired probabilistic feasibility for the UAV.

2. Validation with Random Trials

Given a planned path, we generate random points from the associated distribution, which represent the realization of each obstacle i and the UAV at every time step t. Then we check whether the planned path under the given risk level α for the UAV given in step 1 collides with each realized obstacle i whose center location is generated randomly. Finally, we perform random trials for 100 times for each risk level α under the current case. Count the number of collision occurrence.

A. Case 1: Single Static Uncertain Obstacle + Deterministic UAV

In this case, a static obstacle whose center location obeys a Gaussian distribution is discussed. Fig. 3a shows a sample path generated by standard RRT* without considering chance constraints, while Fig. 3b-3c demonstrate sample paths generated by CC-RRT* at $\alpha = 0.05$. The red line indicates the planned path, the blue circle or ellipse indicates risk bound of the static obstacle, and the yellow circle indicates the realized position of the static obstacle in a random trial. Tab. 1 illustrates that compared with standard RRT* which doesn't consider chance constraints, the proposed CC-RRT* effectively identifies a probabilistically feasible path for the vehicle in the presence of a static, uncertain obstacle. This path can ensure that the probability of collision with the static obstacle at any time step t does not exceed α.

Table 1 Case 1 Simulation Results

Algorithm	α	Avg. Chance of Collision
RRT*	N/A	61%
CC-RRT*	0.20	8%
CC-RRT*	0.10	3%
CC-RRT*	0.05	2%

B. Case 2: Single Static Uncertain Obstacle + Uncertain UAV

In this case, the positions of a static obstacle and a UAV are both considered as uncertain, where the center locations obey the pre-defined Gaussian distributions. Fig. 4a shows a sample path generated by standard RRT* without considering chance constraints, while Fig. 4b-4c depict paths generated by CC-RRT* at risk level $\alpha = 0.05$. Here, the red ellipse indicates the risk domain of the vehicle due to its model uncertainty, others are the same with Case 1. The transformation of relative uncertainty is applied to convert both risk domains of the vehicle and the static obstacle into a common relative risk domain. The simulation results under different risk levels are summarized in Tab. 2, which illustrates that the proposed CC-RRT* can effectively identify a probabilistically feasible path for the vehicle in the presence of both model uncertainty and static environmental sensing uncertainty.

Table 2 Case 2 Simulation Results

Algorithm	α	Avg. Chance of Collision
RRT*	N/A	57%
CC-RRT*	0.20	7%
CC-RRT*	0.10	3%
CC-RRT*	0.05	1%

C. Case 3: Multiple Static Uncertain Obstacles + Uncertain UAV

In this case, three static uncertain obstacles whose centers location obey Gaussian distributions are discussed. Fig. 5a shows the tree generated by CC-RRT*. Fig. 5b depicts paths generated by CC-RRT* at risk level $\alpha = 0.05$. What those different colors indicate are the same with Case 2. The simulation results under different risk levels are

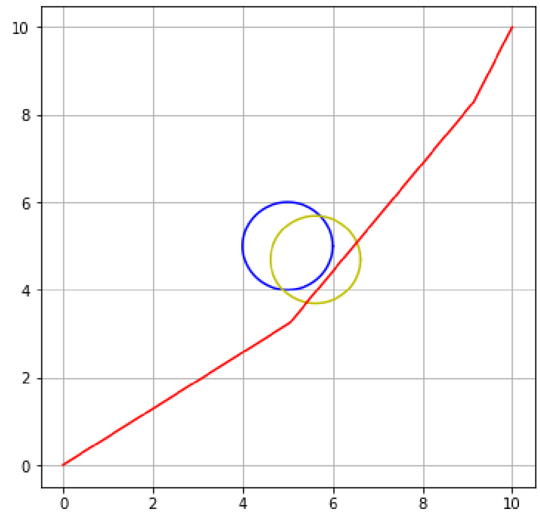

(a) Case 1: standard RRT*

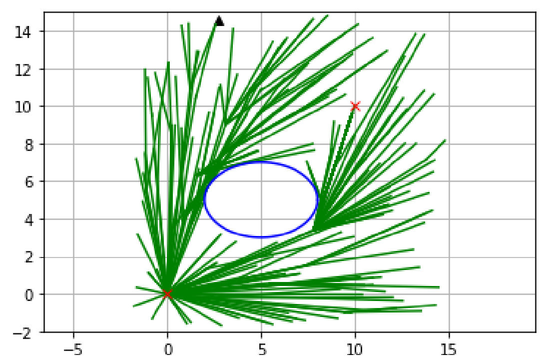

(b) Case 1: tree generated by CC-RRT*

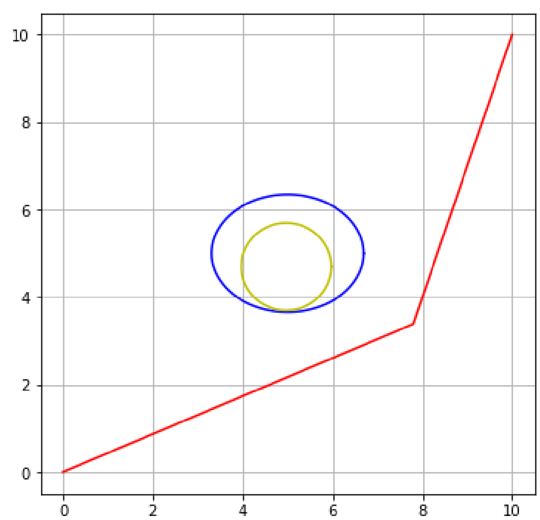

(c) Case 1: CC-RRT*

Fig. 3 Single Static Uncertain Obstacle + Deterministic UAV

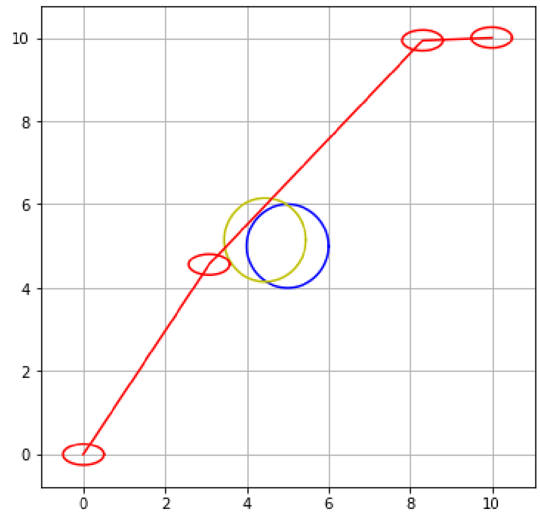

(a) Case 2: Standard RRT*

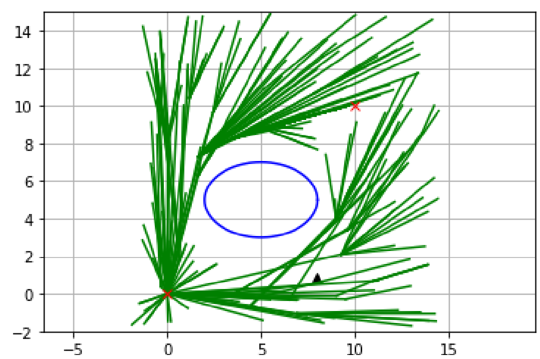

(b) Case 2: tree generated by CC-RRT*

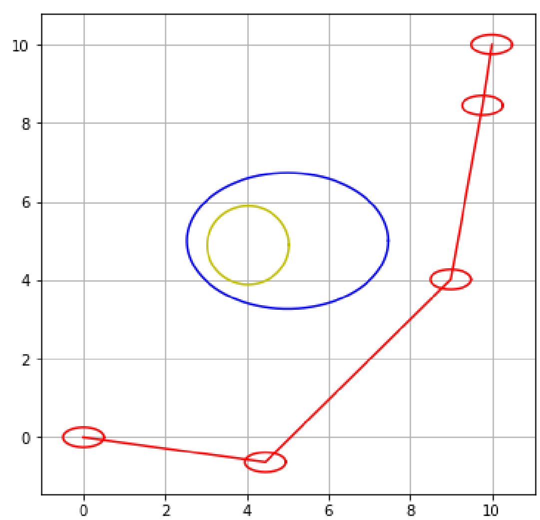

(c) Case 2: CC-RRT*

Fig. 4 Single Static Uncertain Obstacle + Uncertain UAV

summarized in Tab. 3, which illustrates that the proposed CC-RRT* can effectively identify a probabilistically feasible path for the vehicle in the presence of both model uncertainty and multiple static uncertain obstacles.

Table 3 Case 3 Simulation Results

Algorithm	α	Avg. Chance of Collision
RRT*	N/A	76%
CC-RRT*	0.20	7%
CC-RRT*	0.10	4%
CC-RRT*	0.05	2%

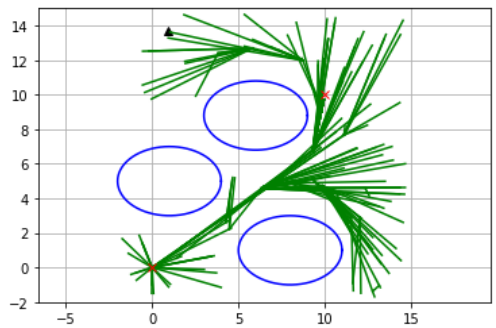

(a) Case 3: tree generated by CC-RRT*

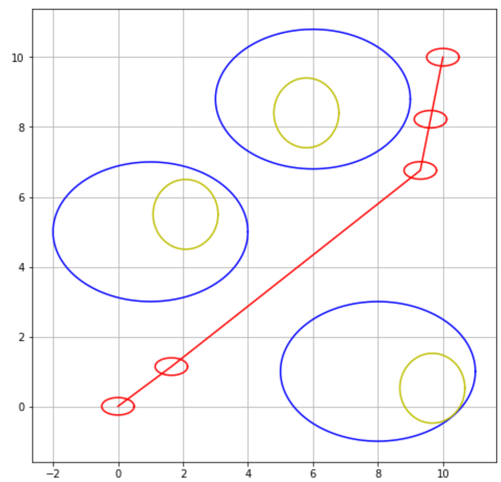

(b) Case 3: CC-RRT*

Fig. 5 Multiple Static Uncertain Obstacles + Uncertain UAV

VI. Conclusions

In this paper, a sampling-based chance constrained RRT* algorithm (CC-RRT*) along with a chance constrained formulation for location uncertainty is presented. Through converting possible regions of obstacles into corresponding risk domains, the probabilistic constraints can be transformed into deterministic ones. Also, by virtue of the introduction of relative uncertainty, this proposed method applies to both model and obstacle uncertainty. Simulation results show that a path for the vehicle satisfying probabilistic feasibility can be identified by the proposed CC-RRT* algorithm with chance constraints formulation.

Acknowledgements

This work was supported by San Diego State University under the University Grants Program.

References

[1] J. Chen and D. Sun, "Stochastic ground-delay-program planning in a metroplex," *Journal of Guidance, Control, and Dynamics*, vol. 41, no. 1, pp. 231–239, 2018.

[2] J. Chen, Y. Cao, and D. Sun, "Modeling, optimization, and operation of large-scale air traffic flow management on spark," *Journal of Aerospace Information Systems*, pp. 504–516, 2017.

[3] D. P. Thipphavong, R. Apaza, B. Barmore, V. Battiste, B. Burian, Q. Dao, M. Feary, S. Go, K. H. Goodrich, J. Homola, *et al.*, "Urban air mobility airspace integration concepts and considerations," in *2018 Aviation Technology, Integration, and Operations Conference*, 2018, p. 3676.

[4] S. M. LaValle, *Planning algorithms*. Cambridge university press, 2006.

[5] S. Thrun, "Probabilistic robotics," *Communications of the ACM*, vol. 45, no. 3, pp. 52–57, 2002.

[6] Y. Yang, J. Zhang, K.-Q. Cai, and M. Prandini, "Multi-aircraft conflict detection and resolution based on probabilistic reach sets," *IEEE Transactions on Control Systems Technology*, vol. 25, no. 1, pp. 309–316, 2016.

[7] S. Prentice and N. Roy, "The belief roadmap: Efficient planning in linear pomdps by factoring the covariance," in *Robotics research*, Springer, 2010, pp. 293–305.

[8] R. Pepy and A. Lambert, "Safe path planning in an uncertain-configuration space using rrt," in *2006 IEEE/RSJ International Conference on Intelligent Robots and Systems*, IEEE, 2006, pp. 5376–5381.

[9] B. Luders, M. Kothari, and J. How, "Chance constrained rrt for probabilistic robustness to environmental uncertainty," in *AIAA guidance, navigation, and control conference*, 2010, p. 8160.

[10] B. D. Luders, G. S. Aoude, J. M. Joseph, N. Roy, and J. P. How, "Probabilistically safe avoidance of dynamic obstacles with uncertain motion patterns," Tech. Rep., 2011.

[11] G. S. Aoude, B. D. Luders, J. M. Joseph, N. Roy, and J. P. How, "Probabilistically safe motion planning to avoid dynamic obstacles with uncertain motion patterns," *Autonomous Robots*, vol. 35, no. 1, pp. 51–76, 2013.

[12] P. Li, M. Wendt, and G. Wozny, "A probabilistically constrained model predictive controller," *Automatica*, vol. 38, no. 7, pp. 1171–1176, 2002.

[13] L. Blackmore, "Robust path planning and feedback design under stochastic uncertainty," in *AIAA Guidance, Navigation and Control Conference and Exhibit*, 2008, p. 6304.

[14] L. Blackmore, H. Li, and B. Williams, "A probabilistic approach to optimal robust path planning with obstacles," in *2006 American Control Conference*, IEEE, 2006, 7–pp.

[15] N. Du Toit, "Robot motion planning in dynamic, cluttered, and uncertain environments: The partially closed-loop receding horizon control approach," PhD thesis, California Institute of Technology, 2010.

[16] B. Gärtner and S. Schönherr, "Smallest enclosing ellipses: An exact and generic implementation in c++," 1998.

[17] S. M. LaValle, "Rapidly-exploring random trees: A new tool for path planning," 1998.

[18] E. Frazzoli, M. A. Dahleh, and E. Feron, "Real-time motion planning for agile autonomous vehicles," *Journal of guidance, control, and dynamics*, vol. 25, no. 1, pp. 116–129, 2002.

[19] Y. Kuwata, J. Teo, G. Fiore, S. Karaman, E. Frazzoli, and J. P. How, "Real-time motion planning with applications to autonomous urban driving," *IEEE Transactions on Control Systems Technology*, vol. 17, no. 5, pp. 1105–1118, 2009.

[20] S. Karaman and E. Frazzoli, "Sampling-based algorithms for optimal motion planning," *The international journal of robotics research*, vol. 30, no. 7, pp. 846–894, 2011.

[21] Y. Liu, "A progressive motion-planning algorithm and traffic flow analysis for high-density 2d traffic," *Transportation Science*, vol. 53, no. 6, pp. 1501–1525, 2019.

[22] R. Vershynin, *High-dimensional probability: An introduction with applications in data science*. Cambridge university press, 2018, vol. 47.

[23] T. A. Snijders, *Multilevel analysis*. Springer, 2011.

[24] J. R. Schott, *Matrix analysis for statistics*. John Wiley & Sons, 2016.